

Article

Quantity Monitor Based on Differential Weighing Sensors for Storage Tank of Agricultural UAV

Junhao Huang ^{1,2,3,4}, Weizhuo He ^{1,2,3,4}, Deshuai Yang ^{1,2,3,4}, Jianqin Lin ^{1,2,3,4}, Yuanzhen Ou ^{1,2,3,4}, Rui Jiang ^{1,2,3,4,*†}  and Zhiyan Zhou ^{1,2,3,4,*†} 

- ¹ Guangdong Laboratory for Lingnan Modern Agriculture, College of Engineering, South China Agricultural University, Guangzhou 510642, China; boulet@stu.scau.edu.cn (J.H.); 15813301373@stu.scau.edu.cn (W.H.); dsyang@stu.scau.edu.cn (D.Y.); 602015148@stu.scau.edu.cn (J.L.); yuanzhenou@stu.scau.edu.cn (Y.O.); ruojiang@scau.edu.cn (R.J.)
- ² Guangdong Provincial Key Laboratory of Agricultural Artificial Intelligence (GDKL-AAI), Guangzhou 510642, China
- ³ Guangdong Engineering Research Center for Agricultural Aviation Application (ERCAAA), Guangzhou 510642, China
- ⁴ Key Laboratory of Key Technology on Agricultural Machine and Equipment, South China Agricultural University, Ministry of Education, Guangzhou 510642, China
- * Correspondence: zyzhou@scau.edu.cn; Tel.: +86-135-6002-6139
- † These authors contributed equally to this work.

Abstract: Nowadays, unmanned aerial vehicles (UAVs) play a pivotal role in agricultural production. In scenarios involving the release of particulate materials, the precision of quantity monitors for the storage tank of UAVs directly impacts its operational accuracy. Therefore, this paper introduces a novel noise-mitigation design for agricultural UAVs' quantity monitors, utilizing differential weighing sensors. The design effectively addresses three primary noise sources: sensor-intrinsic noise, vibration noise, and weight-loading uncertainty. Additionally, two comprehensive data processing methods are proposed for noise reduction: the first combines the Butterworth low-pass filter, the Kalman filter, and the moving average filter (BKM), while the second integrates the Least Mean Squares (LMS) adaptive filter, the Kalman filter, and the moving average filter (LKM). Rigorous data processing has been conducted, and the monitor's performance has been assessed in three UAV typical states: static, hovering, and flighting. Specifically, compared to the BKM, the LKM's maximum relative error ranges between 1.24% and 2.74%, with an average relative error of 0.31%~0.58% when the UAV was in a hovering state. In flight mode, the LKM's maximum relative error varies from 1.68% to 10.06%, while the average relative error ranges between 0.74% and 2.54%. Furthermore, LKM can effectively suppress noise interference near 75 Hz and 150 Hz. The results reveal that the LKM technology demonstrated superior adaptability to noise and effectively mitigates its impact in the quantity monitoring for storage tank of agricultural UAVs.

Keywords: unmanned aerial vehicle (UAV); noise filtering; Butterworth low-pass filter; least mean squares (LMS) adaptive filter; quantity monitoring



Citation: Huang, J.; He, W.; Yang, D.; Lin, J.; Ou, Y.; Jiang, R.; Zhou, Z. Quantity Monitor Based on Differential Weighing Sensors for Storage Tank of Agricultural UAV. *Drones* **2024**, *8*, 92. <https://doi.org/10.3390/drones8030092>

Academic Editor: Pablo Rodríguez-González

Received: 5 January 2024

Revised: 7 February 2024

Accepted: 2 March 2024

Published: 7 March 2024



Copyright: © 2024 by the authors. Licensee MDPI, Basel, Switzerland. This article is an open access article distributed under the terms and conditions of the Creative Commons Attribution (CC BY) license (<https://creativecommons.org/licenses/by/4.0/>).

1. Introduction

In recent years, unmanned aerial vehicles (UAVs) have developed significantly in agricultural production, including application such as scenarios spraying pesticides and herbicides, spreading fertilizers, seeding, and farmland monitoring, etc. [1,2]. Whether the UAV continues to work needs to be determined by judging whether there is still material in the storage tank. The controller unit carried by the UAV needs to determine whether the amount of material currently released is accurate using the mass flow rate. Therefore, it is essential to accurately monitor the allowance and the mass flow rate of the storage tank for the operation accuracy of the UAV in the process of releasing particulate materials [3].

In the existing scientific research, according to the different principles, the monitoring quantity and mass flow rate can be divided into four methods. The first method is the photoelectric method. In the study of this method, Swisher et al. designed an optical sensor for measuring fertilizer flow based on the laser light source. The sensor consisted of 32 photoelectric tubes. The instantaneous flow rate of the fertilizer was obtained according to the shielding strength of particles to light [4]. Grift et al. previously examined the correlation between the output pulse width of the near-infrared photodetector and the fertilizer flow rate. They verified the sensor's detection accuracy at various densities and flow rates. Previously, under high density conditions, they measured the flow rate of spherical granular fertilizer with a diameter of 4.45 mm, achieving a detection error of 3% [5]. Based on the principle of the photovoltaic effect, D. Youchun et al., in 2019, designed a seed flow monitoring device using a thin-surface laser emission module and a silicon photocell, carried out a field sowing test. The test showed that the monitoring accuracy of the device for rape seeds was not less than 98.6%, and the monitoring accuracy of wheat seeds was not less than 95.8% [6]. In a similar context, W. Zaiman et al. used a surface source photoelectric sensor to monitor rice seeds and established a mathematical model between seed number and pulse width, which provided a reference for seed monitoring of precision hill direct seeding of rice [7]. X. Chunji et al. proposed a seeding parameter monitoring method based on a laser sensor and carried out a dust-resistant simulation test, which proved that the laser sensor had stronger dust penetration resistance than the infrared sensor. The monitoring accuracy of the designed monitoring method for double-overlapped seeds can reach 95.4% [8].

The second method is the impact method; the Advanced Farming System of CASE IH Company, Grain-Trak System of the Micro-Trak Company, and Teris System of the Deutz-Fahr Company were all grain-flow monitoring systems based on this method [9]. X. Yingjun et al. previously introduced a digital adaptive interference cancellation method to address the issue of grain flow sensors being susceptible to vibration noise. This method effectively filters out most of the vibration noise, thereby enhancing the sensor's monitoring accuracy [10]. W. Jinwu et al. designed a rice hole direct seeding monitoring system based on the principle of the piezoelectric impact method, which had an effective monitoring accuracy of 97.67%, and the sound and light alarm can be carried out when replaying or missing seedings [11]. W. Shuai used adaptive complementary ensemble empirical mode decomposition wavelet threshold denoising algorithm to denoise the signal of impulse sunflower seed flow sensor. According to the characteristics of sensor voltage signal, the adaptive decomposition is realized. The signal was decomposed into IMF components from high frequency to low frequency. After denoising the high frequency IMF components with low signal-to-noise ratio, the voltage signal which can be used to establish the yield model was obtained [12].

The third method is the capacitance method whose principle is that the capacitance changes with the mass of the plate medium, and the calibration method was used to construct the relationship model between the capacitance value and the seeding rate, so as to realize the monitoring of seed sowing rate. Z. Liming et al. designed a set of seed sowing rate monitoring device this method [13]. C. Jianguo et al. designed a wheat seed number detection system based on a capacitance sensor, established a relationship model between the capacitance value and wheat seed number, and realized seed-number monitoring with a monitoring error of about 2% [14]. Z. Mingyan et al. designed a quantity monitor for a fertilizer storage tank and constructed a relationship model between the fertilizer height and capacitance value based on the capacitance method, which realized the monitoring of fertilizer height [15]. Based on the capacitance method, T. Yanan et al. designed a fertilizer tank level sensor, which realized the effect of on-line monitoring of the fertilizer tank level [16].

The final method is the weighing method. With the rapid development of precision agriculture, weighing sensors have been increasingly used in precision seeding, grain yield monitoring, and quantity monitoring. Al-Jalil et al. designed a weighing sensor device with

adjustable height and width, which was suitable for a variety of agricultural machinery equipment and can realize the weighing of a storage tank [17]. An example of this is the work developed, in 2001, by Van Bergeijk et al., in which a dynamic weighing system for fertilizer applicators was projected. The system included a main weighing sensor and a reference weighing sensor. The reference weighing sensor was used to compensate for the vibration and other signals, which can realize automatic calibration and real-time dynamic weighing [3]. Using a similar approach, Koichi et al. designed a grain yield sensor composed of a ring weighing sensor and an impact plate to realize the real-time estimation of the grain yield [18]. In terms of harvest yield measurements, X. Zhang et al. proposed a method for measuring yield of the harvester based on the weighing method. Short-time wavelet filtering and other methods were used to process flow data in real time. The error of bench test was less than 2%, and the accuracy was good [19]. In terms of fertilization, W. Liguo et al. used the weighing principle to feed back the fertilizer flow information and adjusted the amount of fertilizer in real time according to the speed of the fertilizer applicator to realize the variable fertilizer distribution and fertilization operation, and the fertilization accuracy reached more than 95% [20]. In terms of sowing, L. Haitao et al. designed a seeding rate monitoring system for ground fertilizer applicator based on the weighing sensor. The filtering combination of low-pass filtering + mean filtering + moving average filtering was used to eliminate the mechanical vibration noise. Field experiments showed that the maximum relative error of the monitoring system was 4.88%, and the average relative error was 2.62% [21].

According to the above research, the following results can be obtained; firstly, the monitoring sensor based on the photoelectric method has the advantages of being simple and efficient and having convenient installation. By using the instantaneous flow of the material, the allowance of the material in the storage tank can be calculated. However, it requires a complex calibration process for different materials, and its monitoring accuracy is easily affected by dust. Therefore, it is not suitable for use in a working environment with high dust content. Secondly, the sensors based on the impact method need to construct the relationship model between the flow and impulse. The operation was cumbersome, and the monitoring accuracy was easily affected by the vibration noise. Thirdly, the monitoring device using the capacitance method also needed to calibrate different materials. In addition, the capacitance value was easily affected by environmental factors such as temperature, humidity, and mechanical vibration. It was usually necessary to add a shielding shell around the capacitance plate to reduce the interference of the external environment. And finally, the weighing sensor can directly obtain the allowance of the material and monitor the mass flow. However, in the actual operation process, the body of the agricultural machinery shakes obviously, which easily causes vibration interference of the weighing sensor, resulting in unstable weight data. It is necessary to filter the vibration and noise of the weighing sensor. Therefore, this paper proposed a detection method of the differential weighing sensors with a combination of a measurement sensor and noise sensor to explore the effects of various filtering methods and select a better method.

2. Materials and Methods

2.1. Design of Test Device and Weighing System

2.1.1. Test Device and Circuit Design

The UAV's communication link used in the test included a seeding controller, flight controller, remote controller, UAV ground station, voltage signal conversion module, weighing sensors, and the UAV itself, which is shown in Figure 1. The voltage signal conversion module converts the analog signal of the sensor into a digital signal. It communicates with the seeding controller through USART, the seeding controller communicates with the flight control through USART, and the ground station communicates with the flight control through the Mobile SDK interface. Before the operation, the route was planned, and the seeding parameters were set in the UAV ground station. The ground station uploaded the

route and parameters to the flight controller and seeding controller through the Mobile SDK interface. During the operation, the UAV was seeded according to the set parameters. During the sowing process, the real-time weight of the storage tank displayed on the ground station [22,23].

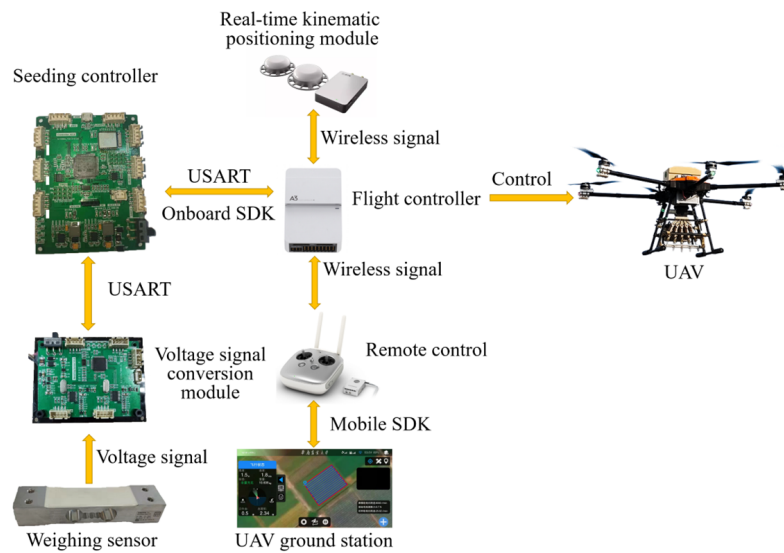


Figure 1. The UAV shot seeding device for test.

The experimental setup used a two-cantilever-beam weighing sensor (Yongkang Jushi Weighing Instrument Co., Ltd., Yongkang, China) monitoring storage tank, and its technical information as shown in Table 1. Generally, an analog-to-digital conversion circuit was used to convert the analog signal into a digital signal, and the single-chip microcomputer read the digital signal. This paper designed an analog-to-digital conversion circuit board using the AD7190 (Analog Devices, Inc., Wilmington, MA, USA), whose technical information is shown in Table 2. The REF3025 voltage reference chip (Texas Instruments, Dallas, TX, USA) was used to provide a precise 2.5 V reference voltage.

Table 1. The technical information of the weighing sensor used in the test.

Range (kg)	Energizing Voltage (V)	Sensitivity (mV/V)	Temperature Range (°C)	Number of Input and Output	Output Signal Type
0~20	2.5~12	2	-20~60	2 and 2	analog

Table 2. The technical information of AD7190.

Number of A/D Converters	Bits	Temperature Range (°C)	Number of Input & Output	Input Signal Type	Output Signal Type
1	24.0	-40~105	2 and 4	analog	digital

2.1.2. Data Processing Scheme

For the noise in the signal, common filtering methods include high-pass filtering, low-pass filtering, band-pass filtering, notch filtering, etc. Such filtering methods need to measure the frequency band of the noise in advance to reduce the noise, and it is difficult to apply to scenes containing a large amount of random noise. The adaptive filter has been widely used in audio processing, power ripple processing, and image processing because of its small amount of calculation, no prior data, good real-time performance, and automatic adjustment of filter coefficients.

In order to reduce the interference of the UAV vibration noise weighing sensor, this paper designed two filtering schemes based on the Least Mean Squares (LMS) adaptive filter and conventional low-pass filter, respectively. The filtering effects of the two schemes were compared through experiments to pick up the suitable filtering scheme of the weighing sensor and provide reliable data for the UAV. The output frequency (filtering frequency) of the data was 250 Hz, and the data processing flow first converts the voltage signal of the weighing sensor into the original weight data, then performs data preprocessing, and finally performs data smoothing. Data processing was a pretreatment with a Butterworth low-pass filter named scheme 1 and with an LMS adaptive filter named scheme 2, as shown in Figure 2. Kalman filtering and moving average filtering were carried out to further reduce the noise in the data and improve the smoothness of the data.

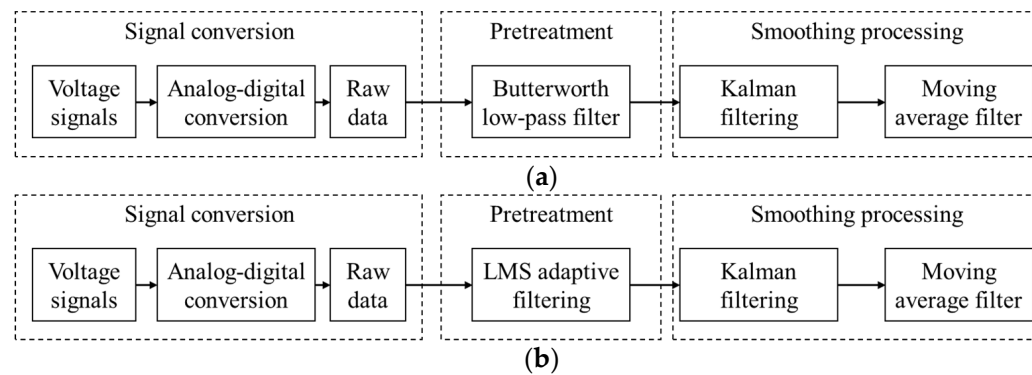


Figure 2. Two data processing schemes: (a) scheme 1 with Butterworth low-pass filter and (b) scheme 2 with LMS adaptive filter.

2.1.3. Differential Weighing Sensors Installation

The installation method of the weighing sensor is shown in Figure 3. Two weighing sensors (No. 1 and No. 2) were used as the main sensors, which were fixed on both sides of the crossbeam of the frame and were used to directly weigh the storage tank. A third weighing sensor (No. 3) was used as a noise monitoring sensor, which was connected to the bottom of the frame beam through a copper column, and the force end of the sensor was fixed to a 500 g counterweight block. When the data processing scheme 1 was adopted, only the data of two main sensors were used; when the data processing scheme 2 was adopted, the data of the two main sensors were used as the reference signal of the LMS adaptive filter, and the data of the noise monitoring sensor were used as the input signal.

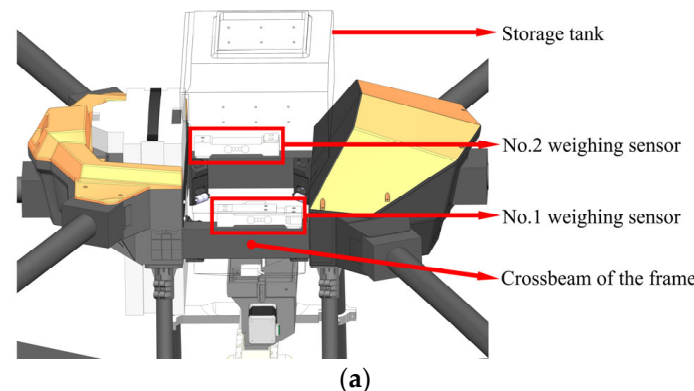


Figure 3. Cont.

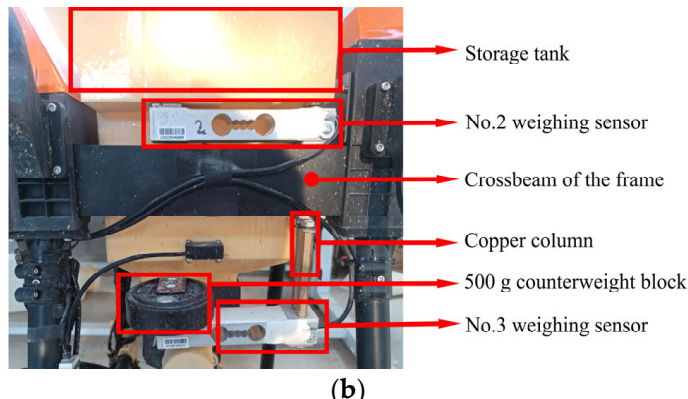


Figure 3. The installation method of differential weighing sensors: (a) the installation of the main sensors and (b) the installation of the noise monitoring sensor.

2.1.4. Filtering Requirements

The filtering requirements were generally considered from two aspects: convergence speed and convergence accuracy, which sometimes contradict each other, that is, increasing the convergence speed (reducing the convergence time) will lead to a convergence accuracy, and reducing the convergence speed (increasing the convergence time) can improve the convergence accuracy. The specific filtering requirements are as follows:

- (1) The weight data mentioned in this paper were mainly used to monitor the storage tank and indicate that there was no material left in the storage tank. The quantity monitor is installed on the UAV and connected to the controller of the UAV. During the operation of the UAV, when the quantity monitor detects that there is nothing remaining in the storage tank, it sent an instruction to the UAV's controller to suspend the operation of the UAV and remind the operator so that the operator can control the UAV to return to the feeding point to add materials, avoiding having the empty storage tank continuing to operate, resulting in missed application. The maximum acceptable error of missed application of the device for the test was 1 m. According to the maximum 3 m/s operating speed of the prototype, the maximum acceptable delay time of the filtered data was 333 ms, that is, the convergence time should be less than 333 ms.
- (2) When the weighing data were used for the judgment of the shortage warning, if the data fluctuation range is large, the accuracy of the shortage warning will be affected. Therefore, the higher the convergence accuracy is, the better. The average relative error of the weighing data during the UAV flight should be less than 3%.

2.2. Data Preprocessing Based on Butterworth Low-Pass Filter

The main feature of the Butterworth filter is that the frequency response curve in its passband has the maximum flatness. The higher the order of the filter, the better the passband characteristics and flatness [24]. The Butterworth low-pass filter can be used to reduce the high-frequency vibration noise in the data. The normalized transfer formula of the n-order Butterworth low-pass filter is as follows [25]:

$$H(s) = \frac{1}{a_0 + a_1 s + a_2 s^2 + a_3 s^3 + \dots + a_n s^n}, \quad (1)$$

where a_0, a_1, a_2, a_3 , and a_n represent polynomial coefficients; n represents the order of the filter. Although increasing the order of the filter can improve the filtering effect, the delay of the filtered data increases, and the amount of calculation becomes larger. Considering both the delay and computational complexity, a second-order Butterworth low-pass filter is selected to preprocess the data, and its normalized transfer formula is as follows:

$$H(s) = \frac{1}{s^2 + 1.414s + 1} \quad (2)$$

Let $P = \tan(\frac{\pi f_d}{f_s})$, the above transfer formula is discretized by bilinear transformation, and s can be transformed into

$$s = \frac{1 - z^{-1}}{1 + z^{-1}}, \quad (3)$$

where f_d represents cut-off frequency, and f_s represents sampling frequency. Replacing (3) in (2)

$$H(z) = \frac{Y(z)}{X(z)} = \frac{P^2 + 2P^2z^{-1} + P^2z^{-2}}{(1 + 1.414P + P^2) + (2P^2 - 2)z^{-1} + (1 - 1.414P + P^2)z^{-2}}, \quad (4)$$

$$Y(z) = b_0 X(z) + b_1 X(z - 1) + b_2 X(z - 2) - a_1 Y(z - 1) - a_2 Y(z - 2), \quad (5)$$

$$b_0 = b_2 = \frac{P^2}{1 + 1.414P + P^2}, \quad (6)$$

$$b_1 = \frac{2P^2}{1 + 1.414P + P^2}, \quad (7)$$

$$a_1 = \frac{2P^2 - 2}{1 + 1.414P + P^2}, \quad (8)$$

$$a_2 = \frac{1 - 1.414P + P^2}{1 + 1.414P + P^2}, \quad (9)$$

where b_0 , b_1 , a_1 , and a_2 represent coefficients of the filter, and the expression in (5) is the final second-order Butterworth low-pass filter data update formula.

By inputting a step signal to the system, the convergence speed of Butterworth low-pass filter is observed to confirm the cut-off frequency and filter coefficient of the filter. The method was to place 10 kg weight on the storage tank. After the weight data are stable, 5 kg of the weight was reduced in an instant, the data change is observed, and the data are recorded before and after filtering at a sampling frequency of 250 Hz when collecting the data.

2.3. Data Preprocessing Based on LMS Adaptive Filtering

The filter mainly included two parts, namely the Finite Impulse Response (FIR) filter and the coefficient update algorithm. The output signal is generated after the input signal passes through the FIR filter, and the error was calculated after the output signal was compared with the desired signal. The coefficient update algorithm adjusted the coefficients of the FIR filter according to the output signal and the error, so that the error gradually became smaller, and then, the adaptive parameter adjustment and filtering were performed.

The main adjustable parameters of the LMS adaptive filtering algorithm were the order k and step factor m . The larger the order, the larger the filter cache, the more data available for the filter reference, but the larger the single calculation; the larger the step size factor, the faster the tracking and convergence speed of the algorithm, but the lower the convergence accuracy. The iterative formula of the LMS adaptive filtering algorithm is [26]

$$\begin{cases} y(n) = b(1)x(n) + b(2)x(n - 1) + b(3)x(n - 2) + \dots + b(k)x(n - k + 1) \\ e(n) = d(n) - y(n) \\ b(k) = b(k - 1) + 2me(n)x(n - k + 1) \end{cases}, \quad (10)$$

where $e(n)$ is the error at time n ; $d(n)$ is the desired signal at time n ; $x(n)$ is the input signal at time n ; $y(n)$ is the output signal at time n ; and $b(k)$ is the k -order filter cache.

The input signal of the LMS adaptive filter is the data of the noise monitoring sensor, the expected signal is the data of the two main sensors, and the output signal is the

filtered data. The data of the main sensor will become smaller and smaller due to the continuous reduction of seed weight during UAV working, and the data can be regarded as a signal source containing noise. The weight of the weight block fixed by the noise monitoring sensor is unchanged, but due to the interference of noise, the data will fluctuate continuously, and the data can be regarded as the noise source. After inputting the data of the main sensor and the noise monitoring sensor into the LMS adaptive filter, the coefficient update algorithm constantly adjusts the coefficients of the FIR filter, gradually eliminates the noise of the main sensor data, and makes the output signal gradually approach the real signal source to realize the data filtering.

The step size factor is the main parameter that affects the convergence speed of the LMS adaptive filter. To determine the size of the step size factor, the order of the filter was fixed to 100. By changing the size of the step size factor, the delay time of the data was observed to analyze the convergence speed. The experimental design is as follows:

- (1) The step size factor was set to 10 levels, ranging from 0.01 to 0.1, and each 0.01 was a level;
- (2) By inputting the step signal into the system, the convergence speed of the filtering algorithm was observed: 10 kg of weight was placed on the storage tank, and 5 kg of weight was reduced in an instant after the weight data were stable, and the data corresponding to different step-size factors were recorded at a sampling frequency of 250 Hz.

2.4. Data Smoothing

2.4.1. Kalman Filtering

As an optimal estimation algorithm [27], the Kalman filter algorithm can filter the observation data with noise. In this paper, the linear Kalman filter algorithm was used to further smooth the data. The algorithm mainly includes two parts: prediction and update. The formula is as follows [28]:

$$\hat{x}_k^- = \hat{x}_{k-1}^- + u_k, \quad (11)$$

$$P_k^- = P_{k-1} + Q, \quad (12)$$

$$K_k = \frac{P_k^-}{P_k^- + R}, \quad (13)$$

$$\hat{x}_k = \hat{x}_k^- + K_k(y_k - \hat{x}_k^-), \quad (14)$$

$$P_k = (I - K_k)P_k^-, \quad (15)$$

In the above formulas, (11) and (12) are the prediction equations of the algorithm, and (13)–(15) are the update equations of the algorithm. Where \hat{x}_k represents the predicted state at time k ; y_k represents the observation at time k ; u_k represents the control effect of the outside world on the system at time k ; P_k represents the covariance matrix at time k ; Q represents the prediction noise matrix; R represents the measurement noise matrix; K_k represents the Kalman gain at time k ; I represents the unit matrix; and \hat{x}_k^- and \hat{P}_k^- represent the corresponding prior variables. When the algorithm is executed, the prior estimation of the state variables is first performed, and the prior covariance is calculated. Then, the Kalman gain is calculated, and finally, the data estimation and covariance update are performed.

When adjusting the parameters of the algorithm, the prediction noise covariance Q and the observation noise covariance R are mainly adjusted. When the Q increases, the dynamic response becomes faster, that is, the convergence speed is accelerated, but the convergence accuracy is reduced. As R increases, the dynamic response becomes slower, that is, the convergence speed becomes slower, but the convergence accuracy is improved. According to the experience of Q and R tuning parameters, there is a final R value of 1.2 and a Q value of 0.1.

2.4.2. Moving Average Filter

In the actual operation process, the frame of the UAV is prone to random vibration, which causes random noise interference to the weight data. Therefore, it is necessary to further smooth the data. The moving average filtering algorithm has the characteristics of simplicity and small computation and can effectively eliminate the random noise in the data and improve the smoothness of the data. The formula is as follows:

$$y(n) = \frac{1}{L} [x(n) + \sum_{t=n-L+1}^n y(t)], \quad (16)$$

where $y(n)$ represents the data after moving average at time n ; $x(n)$ represents the input data at time n ; and L represents the window size of moving average filtering. The window size L determines the filtering effect of the algorithm. When the algorithm is executed, the moving average is calculated after waiting for L data. In theory, the data lags L data. The larger the value of L , the better the filtering effect, but the longer the data delay time.

In this paper, the convergence time of the expected filtering data is less than 333 ms. After the Kalman filter (in Section 2.4.1) is added, the convergence time of the two data processing schemes is 260 ms and 280 ms, respectively. Therefore, after the moving average filtering is added in this section, the convergence time can be extended by 73 ms and 53 ms, respectively. The weight data output frequency of this subject is set to 250 Hz (the filtering period is 4 ms), and the window size should be less than 18.25 and 13.25, respectively, so the window size was 18 and 13, respectively.

2.4.3. Static Filtering Effect

The control system designed in this project had the function of seeding quantity calibration, and the weight data needed to be obtained during calibration. The accuracy requirement of the calibration process for the weight data was a deviation of less than 2 g. The static filtering data were analyzed, the data of 10 s were collected, and the accuracy of the data was evaluated by the average deviation. The average deviation calculation method is as follows:

$$E = \frac{\sum_{n=1}^n |e_n - e_t|}{n}, \quad (17)$$

where E represents the average deviation of the sample (g); e_n represents nth filter data (g); and e_t represents reference weight (g).

2.5. Data Processing Comparison Test

2.5.1. When the UAV Is Hovering

In the hovering state of the UAV, which means that the UAV is stationary in the air, maintaining a certain height and position, the filtering effects of the two data processing schemes were tested, and the design is as follows:

- (1) The test was carried out in sunny conditions with a natural wind speed of less than 3 m/s, and the temperature was between 20 and 28 degrees Celsius. The test site was the open space of the wind tunnel laboratory of South China Agricultural University, Guangzhou, China.
- (2) Before the test, the weight of the storage tank was peeled, and the actual load of the UAV storage tank was changed by adding a 5 kg weight to the storage tank. Five levels of 5, 10, 15, 20, and 25 kg (25 kg is the maximum load) were set up for a total of 5 groups of tests.
- (3) The hovering height of the UAV was set to 1.5 m. At the same time, two filtering schemes were used to filter the original data in real time, and the update rate (output rate) of the filter was 250 Hz. The data were recorded after the UAV hovered stably, and the data recording time was 30 s, that is, 7500 data points were collected.

The actual weight of 5 bags of heavy objects was recorded before the test. The weight was used as the reference weight in the data analysis. The filtered data were compared with the reference weight, and the data were analyzed from the aspects of maximum deviation, maximum relative error, average relative error, and FFT spectrum. The calculation method of the relative error is as follows:

$$\delta_i = \frac{|X_i - X_t|}{X_t} \times 100\% \quad (18)$$

where δ_i represents the relative error of the i th filtered data (kg); X_t represents reference weight (kg). The smaller the relative error, the better the filtering effect. The FFT spectrum can reflect the distribution of noise and the size of noise. The smaller the amplitude corresponding to a certain frequency, the smaller the noise in the data corresponding to that frequency.

Six kinds of filter data were recorded during the experiment. To facilitate chart reading and data analysis, the code shown in Table 3 was used to replace each filter processing.

Table 3. Methods of different filtering processing.

Filter Processing	Code
Butterworth low-pass filter	Treatment 1
LMS adaptive filter	Treatment 2
Butterworth low-pass filter + Kalman filter	Treatment 3
LMS adaptive filter + Kalman filter	Treatment 4
Butterworth low-pass filter + Kalman filter + moving average filter (BKM)	Treatment 5
LMS adaptive filter + Kalman filter + moving average filter (LKM)	Treatment 6

2.5.2. When the UAV Is Flying

In the actual operation process, the UAV was not only in the hovering state, but also in the switching route state and the flight state. However, the UAV was in the flight state most of the time, so the weight data in the flight state were more important. In this test, the corresponding weight data were analyzed when the prototype was in flight, but its actuator was not working. The specific experimental design is as follows:

- (1) The test weather conditions and test sites were the same as those in Section 2.5.1.
- (2) We planned the route at the ground station to make the prototype fly along the route. The working height was set at 1.5 m, and the working speed was set at three levels of 1, 2, and 3 m/s, respectively. The weight of the storage tank was set to 5 levels, which were 5, 10, 15, 20, and 25 kg (25 kg was the maximum load), and a total of 15 groups of tests were carried out.
- (3) At the same time, two filtering schemes were used to filter the weight data in real time, and the update rate (output rate) of the filter was 250 Hz. The data were recorded during the flight of the prototype, and the data recording time was 15 s, that is, 3750 data points were collected.

2.6. UAV Seeding Field Test

To further verify the practical application effect of the treatments, three field tests of rice seeding were carried out in the Mark Village, Dongchong Town, Nansha, Guangzhou, China, the Dagang Village, Zhucun Town, Zengcheng, Guangzhou, China, and the Zengcheng Teaching and Research Base of South China Agricultural University, Guangzhou, China. During the test period, the wind speed was less than 3 m/s, and the temperature was between 22 and 30 degrees Celsius. The test sites and planting features are shown in Figure 4 and Table 4.



Figure 4. The test sites: (a) Mark Village, Dongchong Town, Nansha, Guangzhou, China, (b) Dagang Village, Zhucun Town, Zengcheng, Guangzhou, China, and (c) Zengcheng Teaching and Research Base of South China Agricultural University, Guangzhou, China.

Table 4. UAV seeding field test scheme.

Test Name	Location	Area (hm^2)	Seeding Rate (kg/hm^2)	Row Spacing (m)	Height (m)	Speed (m/s)
Test 1	Mark Village, Dongchong Town, Nansha, Guangzhou, China	0.4453	90	0.25	1.5	2.0
Test 2	Dagang Village, Zhucun Town, Zengcheng, Guangzhou, China	0.1906	150	0.25	1.5	2.0
Test 3	Zengcheng Teaching and Research Base of South China Agricultural University, Guangzhou, China	0.1047	150	0.25	1.5	2.3

In seeding, it was difficult to obtain reliable reference data because the quantity of the storage tank was becoming smaller and smaller. Therefore, the stability of the monitor for the storage tank mainly performed FFT analysis on the data and observed the noise changes before and after filtering to analyze the stability of the monitor for the storage tank.

The weight data of test 1, test 2, and test 3 were recorded and collected at a frequency of 250 Hz when seeding. After the tests, the weight data of three consecutive routes were selected from each test for comparison and analysis.

3. Results

3.1. Determination of Cut-Off Frequency and Filtering Coefficient

Before determining the cut-off frequency, the data needed to be analyzed by Fast Fourier Transform (FFT) to obtain the noise frequency band in the data. When the load of the UAV was about 5 kg, the weight data of the UAV in static was collected, hovering and flight states, and the data acquisition frequency was 250 Hz. The three sets of data were compared and analyzed by FFT using MATLAB® software (R2022a 9.12.0.1884302). The results are shown in Figure 5. The weight data fluctuated less in the stationary state, while the data fluctuated greatly in the hovering and flight states, and the data stability in flight was worse than that in hovering. It can be seen from the FFT spectrum that the noise frequency bands during hovering and flight were widely distributed, and obvious noise interference was generated near the frequencies of 75 and 150 Hz.

Because the noise frequency band was widely distributed and the noise caused great interference to the data, to retain useful low-frequency data, the cut-off frequency was selected at 30 Hz. The stability of the filter was preliminarily verified by using the Filter Designer in MATLAB® software. The response type was selected as ‘Lowpass’, the design method was selected as ‘IIR-Butterworth’, the order was selected as ‘2’, the sampling

frequency was selected as ‘250 Hz’, and the cutoff frequency was selected as ‘30 Hz’. Figure 5 shows that the amplitude–frequency response curve of the filter is a non-oscillatory curve, which met the stability requirements.

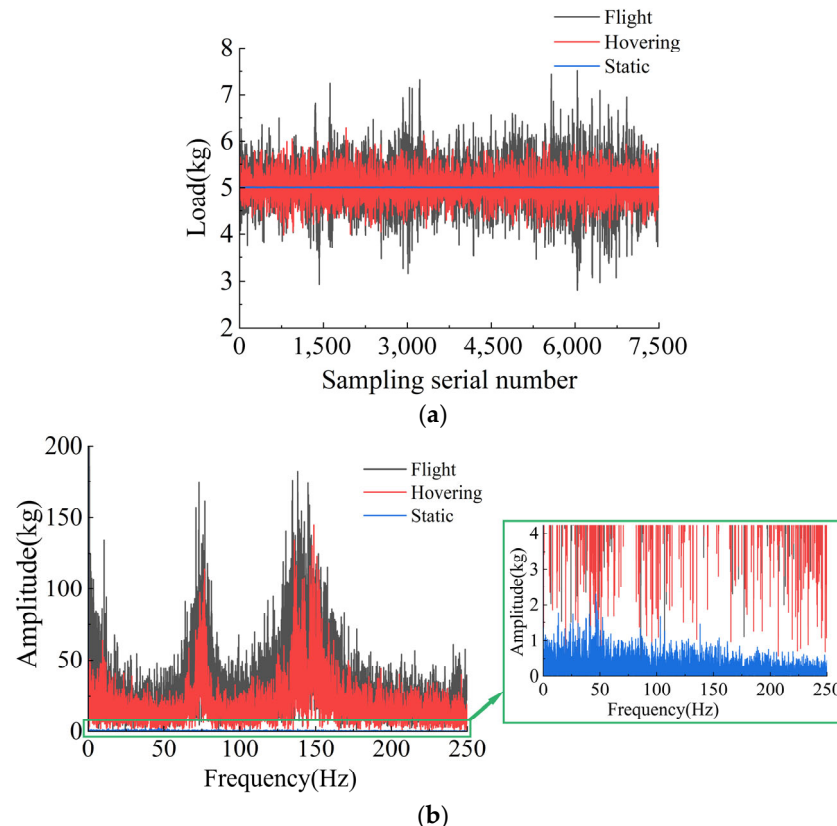


Figure 5. (a) Data comparison and (b) FFT spectrum of UAV in different states.

Using the Filter Designer, the coefficients of the second-order Butterworth low-pass filter are generated. The results were $b_0 = 0.0913$, $b_1 = 0.1826$, $b_2 = 0.0913$, $a_1 = -0.9824$, and $a_2 = 0.3477$.

We input a step signal into the system, and the results are shown in Figure 6.

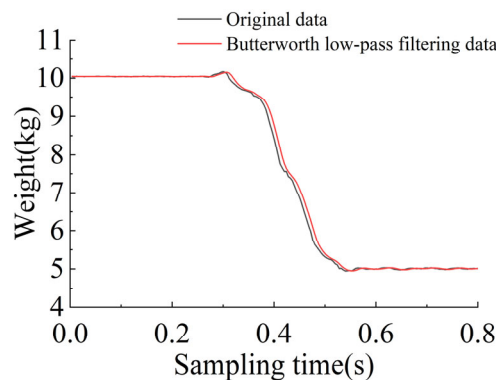


Figure 6. Butterworth low-pass filtering data.

The Butterworth low-pass filtering data lagged behind the original data by about 16 ms, and the convergence time was about 200 ms. The results met the requirement that the convergence time was less than 333 ms. In actual sowing, the instantaneous reduction in the weight of the storage tank by 5 kg was almost non-existent, so the convergence time of the designed Butterworth low-pass filtering algorithm was less than 200 ms.

3.2. Determination of Step Size Factor

For the determination test of the step factor, the weight change is shown in Figure 7. It can be seen from the figure that as the step size factor increased, the convergence speed of the data accelerated. The step size factor started from 0.06, and the growth rate of convergence gradually decreased. Further analysis of the delay time is shown in Table 5. The convergence time corresponding to the step size factors of 0.06, 0.07, 0.08, 0.09, and 0.10 were 294, 255, 222, 216, and 212 ms, respectively, which were within the acceptable convergence time range (less than 333 ms). Since the convergence speed of the step size factor did not change significantly after 0.08, and increasing the step size factor may reduce the convergence accuracy, it was more appropriate to select 0.08 as the step size factor.

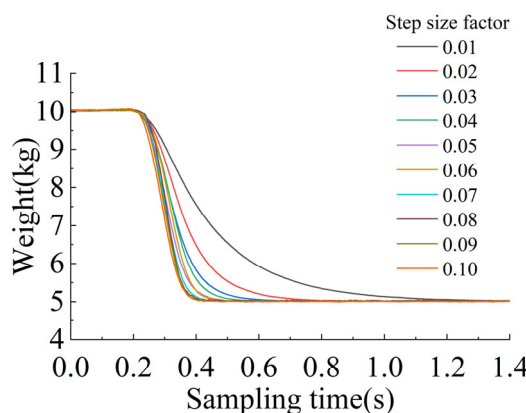


Figure 7. Weight variation in different step size factors.

Table 5. The delay time corresponding to different step size factors.

Step size factor	0.01	0.02	0.03	0.04	0.05	0.06	0.07	0.08	0.09	0.10
Delay time (ms)	1112	720	496	426	343	294	255	222	216	212

3.3. Result of Data Smoothing

3.3.1. Result of Kalman Filtering

By inputting a step signal into the system, the convergence speed of the filtering algorithm was observed. As shown in Figure 8, the data convergence time processed by ‘Butterworth low-pass filtering + Kalman filtering’ was about 260 ms, and the data convergence time processed by ‘LMS self-adaptive filtering + Kalman filtering’ was about 280 ms. The convergence time met the requirements.

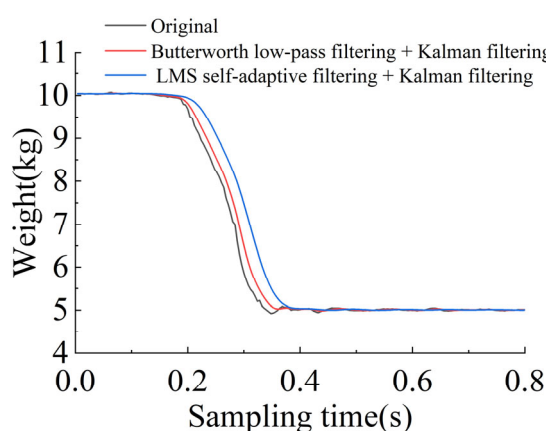


Figure 8. Data comparison after adding Kalman filter.

3.3.2. Result of Moving Average Filter

By inputting a step signal into the system, the convergence speed of the filtering algorithm was observed. The results are shown in Figure 9. The data convergence time processed by BKM was about 318 ms. The data convergence time processed by LKM was about 329 ms, and the convergence time was less than 333 ms, which met the demand. Because this experiment tested the convergence speed of the filtering algorithm by inputting the limit of the step signal (instantaneous reduction of 5 kg), and in the actual UAVs' working, the system input was not a step signal but generally a skew signal, the filtering algorithm convergence speed will be faster, and the convergence time will be shorter.

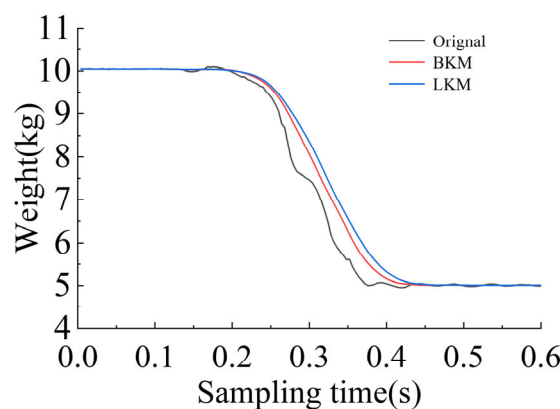


Figure 9. Increase in the data comparison after moving average filtering.

3.3.3. Result of Static Filtering Effect

The experimental results are shown in Figure 10 and Table 6. The average deviation of the data processed by BKM was 1.41 g. The average deviation of the data processed by LKM was 1.47 g, and the average deviation of the original data was 4.79 g. The two data processing schemes had a better filtering effect in the static state, which can meet the accuracy requirements of sowing quantity calibration.

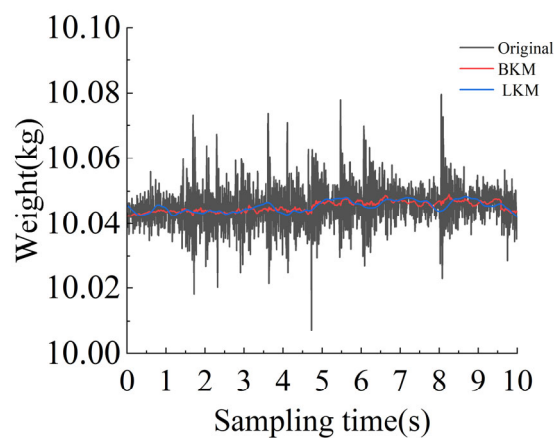


Figure 10. Static filtering data comparison.

Table 6. The average deviation of data in static state.

Filter Processing	Average Deviation (g)
Original	4.79
BKM	1.41
LMS	1.47

3.4. Data Processing Comparison Result When the UAV Was Hovering

After different filtering processing under different loads, the data pair is shown in Figure 11. It can be seen from the figure that under the five load levels, the original weight data without filtering fluctuates greatly. This is due to the vibration of the frame when the UAV was hovering. In addition, the UAV was not kept at the same height, and the UAV continued to move up and down at the target height. The vibration generated by the frame was transmitted to the storage tank, which ultimately caused the measurement result of the weighing sensor to be unstable.

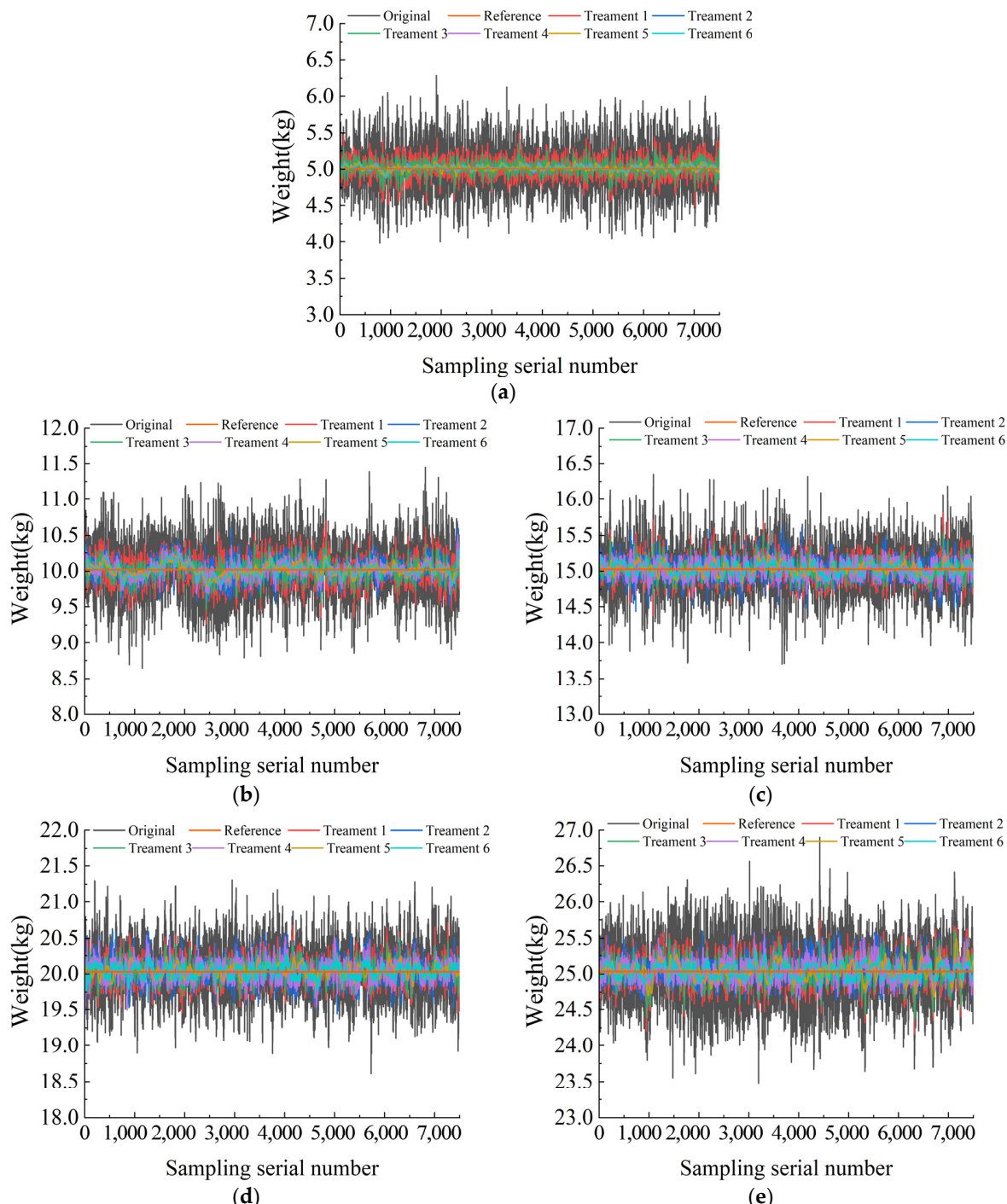


Figure 11. Comparison of processing data under different loads: (a) 5 kg, (b) 10 kg, (c) 15 kg, (d) 20 kg, and (e) 25 kg.

The data are further analyzed to calculate the maximum deviation, the maximum relative error, and the average relative error. The results are shown in Table 7. When the UAV was loaded with 5, 10, 15, 20 and 25 kg, respectively, the maximum deviations of the original data were 1.574, 1.690, 1.380, 1.522, and 1.872 kg, respectively, indicating that the unfiltered data had a large deviation and was difficult to use directly. After Treatment 5 and 6, the maximum deviation of the original data was less than 0.5 kg.

Table 7. Maximum relative error, average relative error, and standard deviation.

Load (kg)	Filter Processing	Maximum Deviation (kg)	Maximal Relation Error (%)	Mean Relative Deviation (%)
5	Original data	1.574	31.48	4.80
	Treatment 1	0.779	15.58	1.84
	Treatment 2	0.138	2.76	0.66
	Treatment 3	0.513	10.26	1.24
	Treatment 4	0.125	2.50	0.62
	Treatment 5	0.146	2.92	0.66
	Treatment 6	0.108	2.16	0.58
10	Original data	1.690	16.90	2.61
	Treatment 1	0.753	7.53	1.26
	Treatment 2	0.603	6.03	1.00
	Treatment 3	0.562	5.62	0.82
	Treatment 4	0.491	4.91	0.70
	Treatment 5	0.246	2.46	0.57
	Treatment 6	0.274	2.21	0.49
15	Original data	1.380	9.20	1.55
	Treatment 1	0.784	5.23	0.77
	Treatment 2	0.641	4.27	0.69
	Treatment 3	0.500	3.33	0.55
	Treatment 4	0.409	2.73	0.53
	Treatment 5	0.275	1.83	0.38
	Treatment 6	0.172	1.15	0.47
20	Original data	1.522	7.61	1.39
	Treatment 1	0.755	3.78	0.64
	Treatment 2	0.608	3.04	0.59
	Treatment 3	0.546	2.73	0.48
	Treatment 4	0.587	2.94	0.49
	Treatment 5	0.251	1.26	0.34
	Treatment 6	0.232	1.16	0.33
25	Original data	1.872	7.49	1.18
	Treatment 1	0.866	3.46	0.60
	Treatment 2	0.576	2.30	0.42
	Treatment 3	0.672	2.69	0.47
	Treatment 4	0.587	2.35	0.34
	Treatment 5	0.464	1.86	0.36
	Treatment 6	0.310	1.24	0.31

The filtered data of Treatment 5 and Treatment 6 are further analyzed, and the FFT spectrum diagram is drawn as shown in Figure 12.

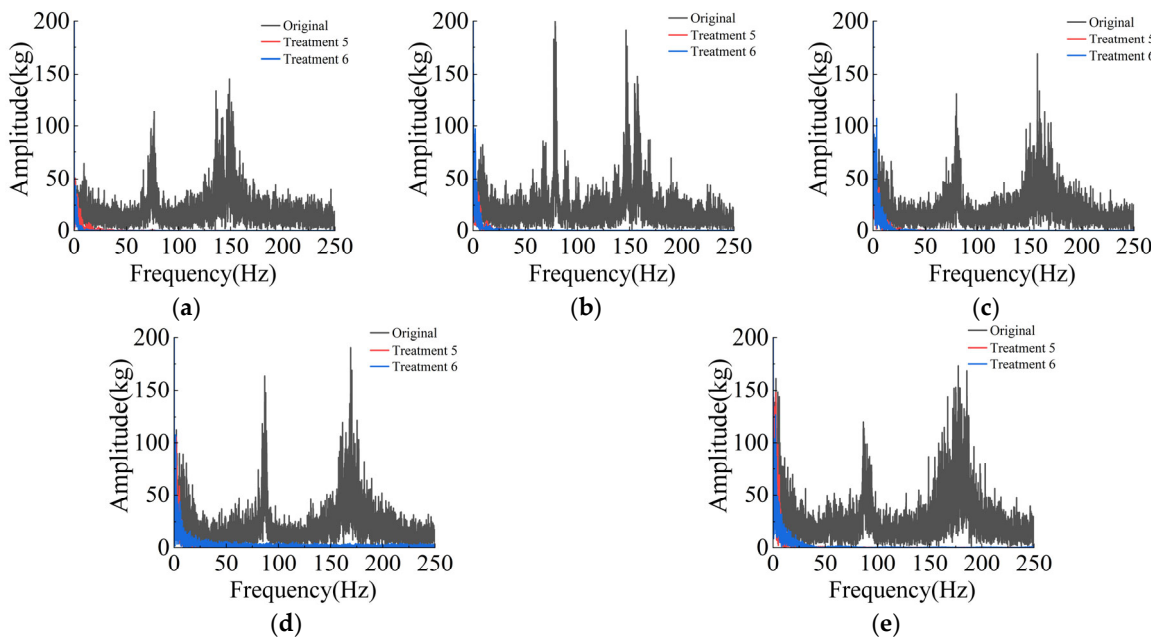


Figure 12. FFT spectrum of each processing data under different loads: (a) 5 kg, (b) 10 kg, (c) 15 kg, (d) 20 kg, and (e) 25 kg.

3.5. Data Processing Comparison Result When the UAV Was Flighting

Section 3.4 has analyzed each processing, indicating that the filtering effect of Treatment 5 and Treatment 6 was better. Therefore, when analyzing the weight data of flight, this section focuses on comparing the data of Treatment 5 and Treatment 6. The filtered data waveform is shown in Figure 13.

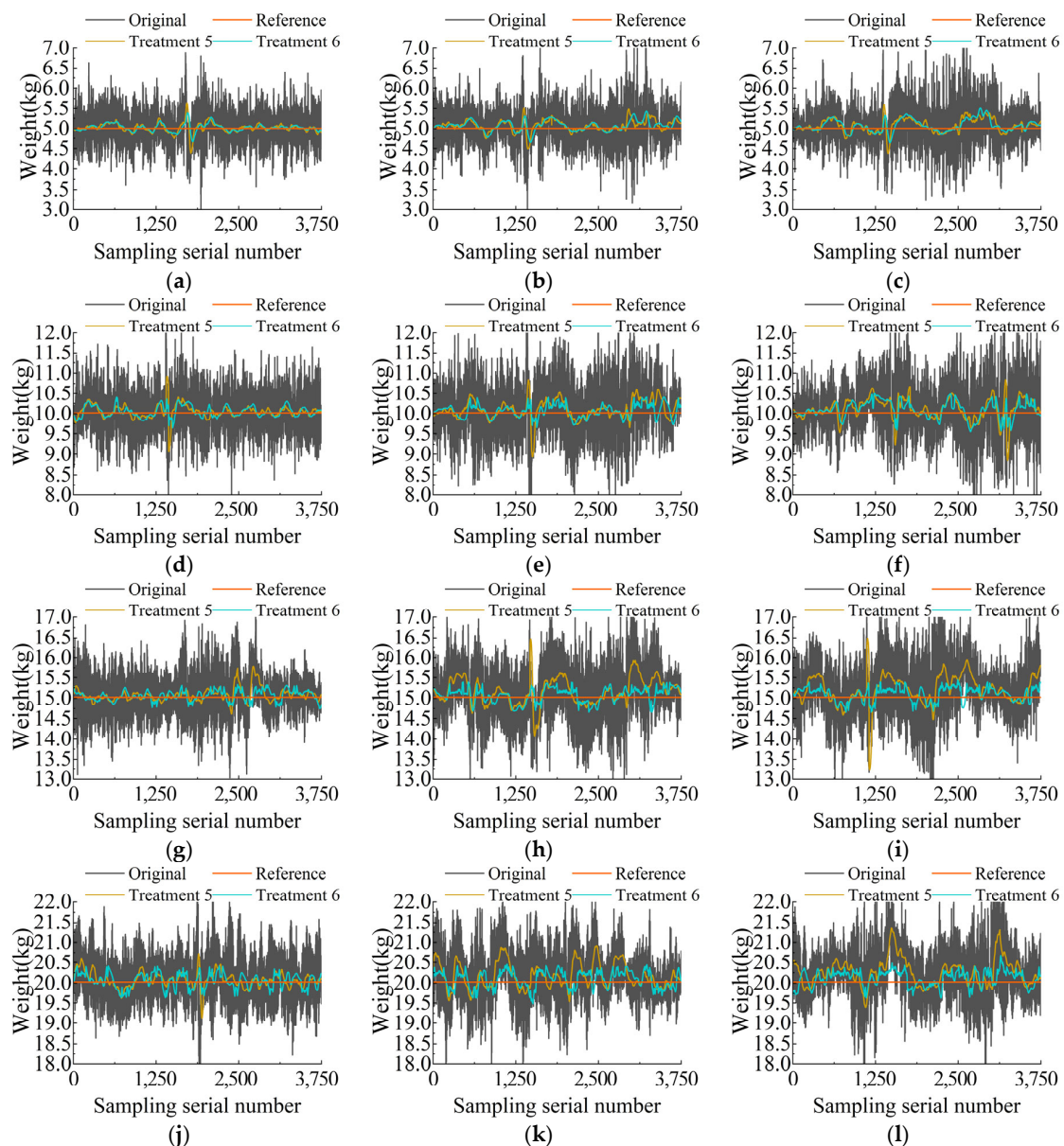
Further analyzing the above data, the statistical maximum deviation, maximum relative error, and average relative error are shown in Table 8.

Table 8. Corresponding results of different loads and different operating speeds.

Evaluating Indicator	Filter Processing	Speed (m/s)	Load (kg)				
			5	10	15	20	25
Maximum deviation (kg)	Original data	1	1.995	2.924	2.201	2.669	2.427
		2	2.316	2.584	2.417	2.587	2.552
		3	2.654	3.136	2.547	3.103	3.666
	Treatment 5	1	0.642	0.943	0.763	0.901	1.064
		2	0.515	1.088	1.448	0.895	1.503
		3	0.621	1.173	1.799	1.329	2.031
Maximal relation error (%)	Treatment 6	1	0.381	0.391	0.306	0.396	0.420
		2	0.425	0.392	0.368	0.546	0.817
		3	0.503	0.484	0.427	0.654	0.888
	Original data	1	39.90	29.24	14.67	13.35	9.71
		2	46.32	25.84	16.11	12.94	10.21
		3	53.08	31.36	16.98	15.52	14.66
	Treatment 5	1	12.84	9.43	5.09	4.51	4.26
		2	10.30	10.88	9.65	4.48	6.01
		3	12.42	11.73	11.99	6.65	8.12
	Treatment 6	1	7.62	3.91	2.04	1.98	1.68
		2	8.50	3.92	2.45	2.73	3.27
		3	10.06	4.84	2.85	3.27	3.55

Table 8. Cont.

Evaluating Indicator	Filter Processing	Speed (m/s)	Load (kg)				
			5	10	15	20	25
Mean relative deviation (%)	Original data	1	6.94	4.35	2.77	2.34	1.67
		2	7.30	5.37	3.65	2.54	2.23
		3	7.90	5.39	3.71	2.77	2.62
	Treatment 5	1	1.64	1.11	0.75	0.72	0.82
		2	2.40	1.87	1.85	1.31	1.61
		3	2.86	2.21	2.02	1.55	1.96
	Treatment 6	1	1.38	1.13	0.74	0.78	0.76
		2	2.32	1.43	1.09	0.97	1.13
		3	2.54	1.79	1.10	0.92	1.37

**Figure 13.** Cont.

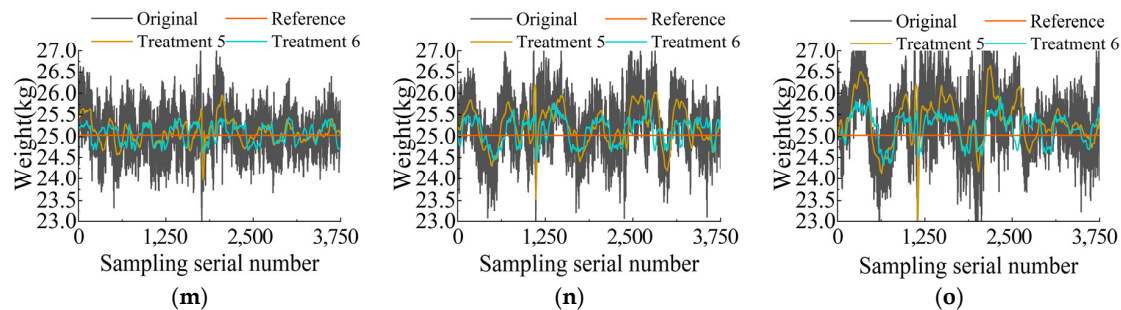


Figure 13. Data comparison under different loads and different flight speeds: (a–c) 5 kg (1~3 m/s), (d–f) 10 kg (1~3 m/s), (g–i) 15 kg (1~3 m/s), (j–l) 20 kg (1~3 m/s), and (m–o) 25 kg (1~3 m/s).

3.6. Result of Field Tests

The data of field tests and result of the FFT analysis are shown in Figure 14.

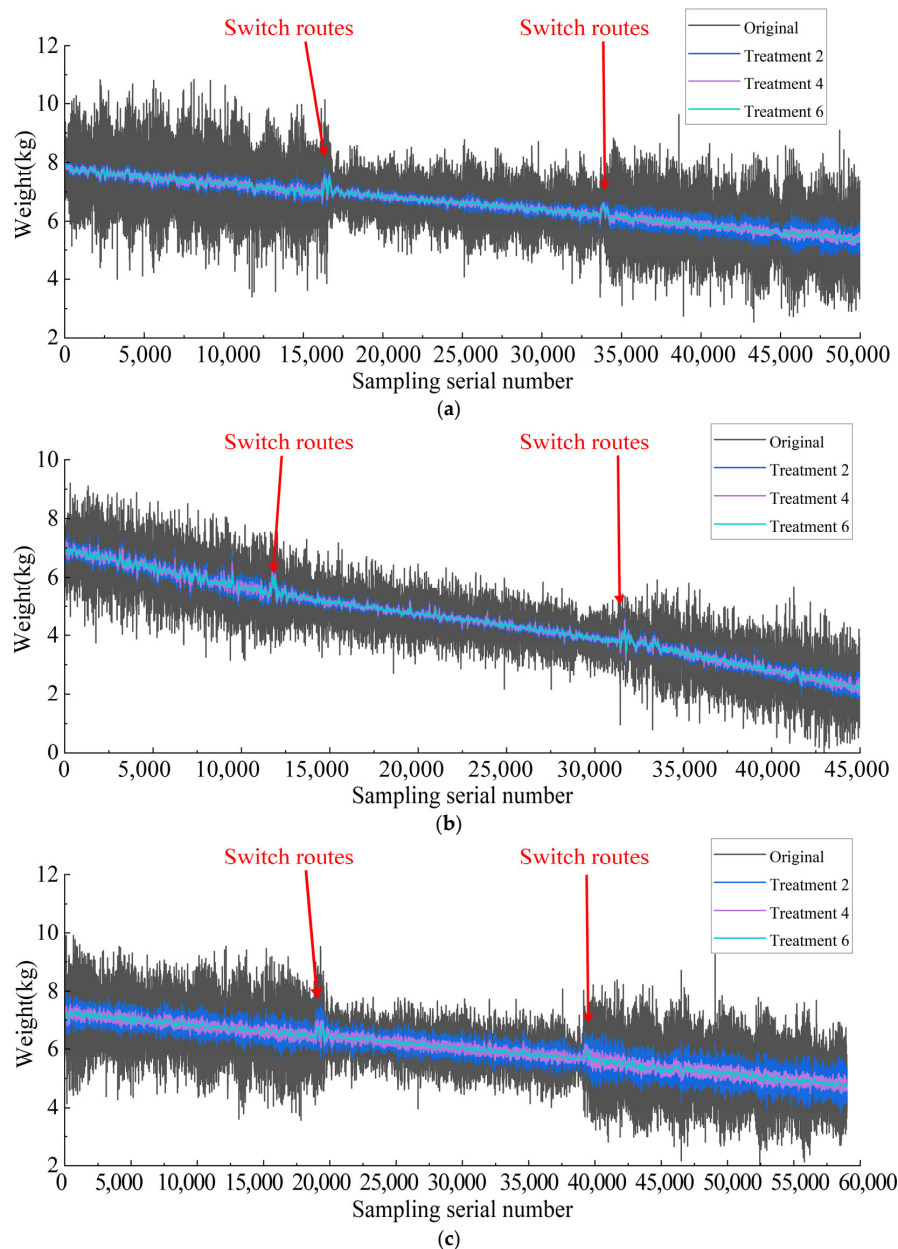


Figure 14. Cont.

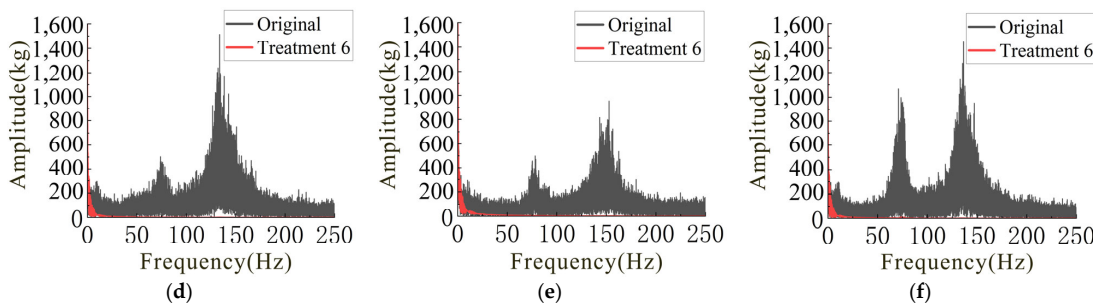


Figure 14. Data of field tests: (a) test 1, (b) test 2, and (c) test 3; and results of FFT analysis: (d) test 1, (e) test 2, and (f) test 3.

4. Discussion

4.1. Analysis of UAV Hovering Test

It can be seen from Figure 11 that the unfiltered original weight data fluctuate greatly at five load levels. This is due to the vibration of the frame when the UAV was hovering. In addition, the UAV was not kept at the same height, and the UAV continued to move up and down at the target height. The vibration generated by the frame was transmitted to the storage tank, which ultimately caused the measurement result of the weighing sensor to be unstable.

After processing 1 and processing 2, the amplitude of data fluctuation was significantly reduced. Under the load of 5, 10, and 15 kg, the data fluctuation amplitude of treatment 2 was less than that of treatment 1, while under the load of 20 and 25 kg, the data fluctuation amplitude of treatment 1 and treatment 2 was similar, which proves that the filtering effect of treatment 2 was better than that of treatment 1, and the adaptability of treatment 2 was stronger. The reason for this phenomenon may be that under different loads, the vibration of the frame was irregular, and the generated vibration noise was random. Processing 1 set a fixed cut-off frequency, which made it difficult to effectively eliminate random noise. Processing 2 continuously adjusted the coefficient of the filter during execution and had an adaptive adjustment ability, which can better filter out random noise.

After the original data were processed by processing 3 and processing 4, respectively, the amplitude of data fluctuation was further reduced, and the filtering effect was better than that of processing 1 and processing 2, respectively, indicating that the Kalman filter algorithm can effectively reduce the noise and further eliminate the random noise. After the original data were processed by processing 5 and 6, respectively, the amplitude of data fluctuation was further reduced, and the filtering effect was better than that of processing 3 and 4, respectively, which shows that the moving average filtering had a better noise reduction ability and can improve the smoothness of the data.

Table 7 shows that there was a large deviation in the unfiltered data, which was difficult to use directly. After processing 5 and 6, the maximum deviation of the original data was less than 0.5 kg, but under the same load, the maximum deviation of processing 6 was smaller. With the increase in load, the maximum deviation of treatment 5 and treatment 6 became larger, which indicated that the larger the load, the larger the noise generated by the UAV frame and the larger the deviation. From the perspective of maximum relative error, the maximum relative error of the original data after processing 5 was 1.26~2.94%, while the maximum relative error after processing 6 was 1.24~2.74%, indicating that under the same load, the maximum relative error of processing 6 was smaller, so the filtering effect of processing 6 was better. From the perspective of average relative error, the average relative error of the original data was within 1.18~4.80%, the average relative error of treatment 5 was within 0.34~0.66%, and the average relative error of treatment 6 was within 0.31~0.58%, indicating that treatment 5 and treatment 6 had a better filtering effect and met the filtering requirements.

It can be seen from Figure 12 that a large amount of noise was mixed in the original data. Near the frequencies of 75 and 150 Hz, the fluctuation range of the original data was

large, and the noise interference to the data was more serious. After processing 5 and 6, the amplitude corresponding to the same frequency was reduced by about 100 orders of magnitude, and the noise was well suppressed.

4.2. Analysis of UAV Flighting Test

It can be seen from Figure 13, under the same load, with the increase in working speed, the fluctuation range of data became larger. This is because the greater the speed, the greater the vibration amplitude of the frame, and the greater the noise. At the same operating speed, with the increase in load, the fluctuation range of data became larger, indicating that the noise increases with the increase in load. By comparing the data waveforms of processing 5 and processing 6, it can be seen that the data waveform of processing 5 fluctuates less when the load was 5 and 10 kg, but the fluctuation became larger when the load was 15, 20, and 25 kg, while the data of processing 6 fluctuate slightly near the reference data, which shows that processing 6 encounters larger vibration and noise, better stability, stronger adaptability, and better filtering effect.

In Table 8, the maximum deviation range of the original data was 1.995~3.666 kg. Overall, the deviation is larger than the original data of the hovering test in Section 3.4, indicating that the vibration noise of the UAV during flight was larger than that during hovering. With the increase in load and working speed, the maximum deviation of treatment 5 and treatment 6 gradually becomes larger. When the load was 25 kg, the deviation increases obviously. Currently, the maximum deviation of treatment 5 was in the range of 1.064~2.031 kg, and the maximum deviation of treatment 6 is in the range of 0.420~0.888 kg. In contrast, treatment 6 had a better noise suppression ability.

From the perspective of relative error, the maximum relative error of treatment 5 was 4.26~12.84%, and the average relative error was 0.72~2.86%. The maximum relative error of treatment 6 was 1.68~10.06%, and the average relative error was 0.74~2.54%, which all met the filtering requirements. Under the same conditions, the maximum relative error and average relative error of treatment 6 were smaller than those of treatment 5, which shows that treatment 6 has a better noise suppression ability and smoother data filtering data.

4.3. Analysis of Field Test

Figure 14 shows that the original data are seriously disturbed by the vibration and noise of the UAV, and the data fluctuate in a large range. After processing 2 (LMS adaptive filtering), the stability of the data is greatly improved. After the original data were processed by processing 4 (LMS adaptive filtering + Kalman filtering), the fluctuation range of the data was reduced again, and the noise was further filtered out. After the original data were processed by processing 6 (LKM), the data were smoother, the stability was better, and the noise was effectively suppressed. The data fluctuation range of test 3 was larger than that of test 1 and test 2, because the working speed of test 3 was faster than that of test 1 and test 2. The faster the working speed, the greater the vibration noise and the more unstable the data.

Further analysis shows that when the UAV switches the route, the data had a large fluctuation. The possible reason was that during the switching route, the gravity acceleration of the UAV changed drastically, and the UAV switched continuously in the two states of overweight and weightlessness, resulting in the continuous shaking of the storage tank and the large-scale fluctuation of the data.

The FFT analysis in Figure 14 shows that the frequency band of noise was widely distributed before filtering, and the noise interference was more serious near the frequency of 75 Hz and 150 Hz. After filtering, the amplitude corresponding to the same frequency was reduced by about 1000 orders of magnitude, and the noise near 75 Hz and 150 Hz was effectively suppressed.

4.4. A Comparison with Existing Research

Obtaining the allowance in the storage tank is very important for various devices in agricultural production and is a key factor in improving the working accuracy of the devices [29,30]. In the existing research, the filtering processing of weighing data is often limited to the use of a single filter. This paper innovatively proposes a new processing scheme, that is, multiple filters optimized for different noise types are continuously applied. In order to verify the effectiveness of this scheme, this paper compares several groups of experiments and finds a better filter combination to further improve the accuracy and effect of data processing. Through this continuous filtering method, it can filter out all kinds of noise interference more comprehensively, so as to obtain more accurate and reliable weighing data.

The final filtering scheme adopts the LMS adaptive filtering scheme with fixed step size factor, but the fixed step size factor is difficult to balance with the steady-state error and convergence speed. In order to further improve the filtering effect, the variable-step-size LMS adaptive filtering algorithm can be used in subsequent research [31]. In addition, compared with existing schemes, a noise monitoring sensor is added to the final determined storage tank allowance monitoring scheme, which means an increase in cost and an increase in installation difficulty. Other schemes can also be tried to further improve the stability and reliability of seed box allowance monitoring data [32].

5. Conclusions

In this paper, aiming to evaluate the influence of UAV's vibration noise in the accurate quantity weighing of the storage tank, a differential sensor and supporting two filtering methods with strong adaptability were provided to filter out the noise. The quantitative evaluation was summarized as follows:

- (1) The analog-to-digital conversion circuit for reading the weighing sensor signal was designed, and two data processing schemes were proposed, which are Butterworth low-pass filter + Kalman filter + moving average filter (BKM) and LMS adaptive filter + Kalman filter + moving average filter (LKM).
- (2) The UAV hovering test was carried out, and two data processing schemes were compared. The results show that for different loads, the scheme of LKM can effectively suppress noise. The maximum relative error of the filtered data is 1.24~2.74%, and the average relative error is 0.31~0.58%.
- (3) The results of the UAV flight test show that for different loads and different flight speeds, the LKM has a better noise suppression ability and better filtering effect than the BKM. The maximum relative error of the filtered data is 1.68~10.06%, and the average relative error is 0.74~2.54%.

Author Contributions: Writing—original draft preparation, J.H.; methodology and validation, W.H.; investigation, D.Y.; data curation, J.L.; visualization, Y.O.; writing—review and editing, R.J.; conceptualization, Z.Z. All authors have read and agreed to the published version of the manuscript.

Funding: This work was supported by the Laboratory of Lingnan Modern Agriculture Project (NT2021009), the Project of key R&D program of Guangzhou of China (202206010149), in part by Science and Technology Plan of Jian City of China (20211-055316 and [2020]83), Science and Technology Plan of Jian City of China (2022-051252-02), Science and Technology Plan of Guangdong Province of China (2023B10564002 and 2021B1212040009), Innovative Research Team of Agricultural and Rural Big Data in Guangdong Province of China (2019KJ138), and China Scholarship Council (202308440394).

Data Availability Statement: Data are contained within the article.

Conflicts of Interest: The authors declare no conflicts of interest.

References

1. Kim, J.; Kim, S.; Ju, C.; Son, H.I. Unmanned Aerial Vehicles in Agriculture: A Review of Perspective of Platform, Control, and Applications. *IEEE Access* **2019**, *7*, 105100–105115. [[CrossRef](#)]
2. Rejeb, A.; Abdollahi, A.; Rejeb, K.; Treiblmaier, H. Drones in agriculture: A review and bibliometric analysis. *Comput. Electron. Agric.* **2022**, *198*, 107017. [[CrossRef](#)]
3. van Bergeijk, J.; Goense, D.; van Willigenburg, L.G.; Speelman, L. PA—Precision Agriculture. *J. Agric. Eng. Res.* **2001**, *80*, 25–35. [[CrossRef](#)]
4. Swisher, D.W.; Borgelt, S.C.; Sudduth, K.A. Optical sensor for granular fertilizer flow rate measurement. *Trans. ASAE* **2002**, *45*, 881–888. [[CrossRef](#)]
5. Grift, T.E.; Walker, J.T.; Hofstee, J.W. Mass flow measurement of granular materials in aerial application. Part 2: Experimental model validation. *Trans. ASAE* **2001**, *44*, 27–34. [[CrossRef](#)]
6. Ding, Y.; Wang, K.; Du, C.; Liu, X.; Chen, L.; Liu, W. Development of monitoring device for medium and small size seed flow based on thin surface laser-silicon photocell. *Trans. Chin. Soc. Agric. Eng.* **2019**, *35*, 12–20. [[CrossRef](#)]
7. Wang, Z.; Pei, J.; He, J.; Zhang, M.; Yang, W.; Luo, X. Development of the sowing rate monitoring system for precision rice hill-drop drilling machine. *Trans. Chin. Soc. Agric. Eng.* **2020**, *36*, 9–16. [[CrossRef](#)]
8. Xie, C.; Zhang, D.; Yang, L.; Cui, T.; He, X.; Du, Z. Seeding parameter monitoring method based on laser sensors. *Trans. Chin. Soc. Agric. Eng.* **2021**, *37*, 140–146. (In Chinese)
9. Wang, S.; Yu, Z.; Zhang, W.; Yang, L.; Zhang, Z.; Ao, R. Review of recent advances in online yield monitoring for grain combine harvester. *Trans. Chin. Soc. Agric. Eng.* **2021**, *37*, 58–70. [[CrossRef](#)]
10. Xiong, Y.; Zhou, J.; Wei, W.; Shen, M.; Zhang, B. Design and experiment of grain mass flow sensor based on embedded system. *Trans. Chin. Soc. Agric. Eng.* **2018**, *34*, 39–46. [[CrossRef](#)]
11. Wang, J.; Zhang, Z.; Wang, F.; Jiang, Y.; Zhou, W. Design and Experiment of Monitoring System for Rice Hill-direct-seeding Based on Piezoelectric Impact Method. *Trans. Chin. Soc. Agric. Mach.* **2019**, *50*, 74–84, 99. [[CrossRef](#)]
12. Wang, S. Study on Design and Key Technology for Sunflower Combine Harvester Online Yield Monitor System Based on Pneumatic Conveying Structure. Ph.D. Thesis, Inner Mongolia Agricultural University, Hohhot, China, 2022. (In Chinese)
13. Zhou, L.; Ma, M.; Yuan, Y.; Zhang, J.; Dong, X.; Wei, C. Design and test of fertilizer mass monitoring system based on capacitance method. *Trans. Chin. Soc. Agric. Eng.* **2017**, *33*, 44–51. [[CrossRef](#)]
14. Chen, J.; Li, Y.; Qin, C.; Liu, C. Design and Experiment of Precision Detecting System for Wheat-planter Seeding Quantity. *Trans. Chin. Soc. Agric. Mach.* **2019**, *50*, 66–74. [[CrossRef](#)]
15. Zhao, M.; Wang, X.; Qi, Z.; Tian, Y. Design and Test of Material Level Detection Sensor for Fertilizer Box Based on Capacitance Method. *J. Agric. Mech. Res.* **2019**, *41*, 151–155. [[CrossRef](#)]
16. Tian, Y.; Qi, Z.; Wang, X.; Zhao, M. Design and Experiment of Material Level Sensor for Fertilizer Tank Based on Single Chip Microcomputer. *J. Agric. Mech. Res.* **2020**, *42*, 105–110. [[CrossRef](#)]
17. Al-Jalil, H.F.; Khair, A.; Mukahal, W. Design and performance of an adjustable three-point hitch dynamometer. *Soil Till Res* **2001**, *62*, 153–156. [[CrossRef](#)]
18. Shoji, K.; Itoh, H.; Kawamura, T. A Mini-grain Yield Sensor Compensating for the Drift of its Own Output. *Eng. Agric. Environ. Food* **2009**, *2*, 44–48. [[CrossRef](#)]
19. Zhang, X.C.; Hu, X.; Zhang, A.G.; Zhang, Y.; Yuan, Y. Method of measuring grain-flow of combine harvester based on weighing. *Trans. Chin. Soc. Agric. Eng.* **2010**, *26*, 125–129.
20. Wei, L.; Zhang, X.; Yuan, Y.; Liu, Y.; Li, Z. Design and experiment of 2F-6-BP1 variable rate assorted fertilizer applicator. *Trans. Chin. Soc. Agric. Eng.* **2012**, *28*, 14–18. [[CrossRef](#)]
21. Liu, H.; Ding, Y.; Yu, H.; Jin, M.; Jiang, Y.; Fu, X. Signal processing method and performance tests on weighting-sensor-based measuring system of output quantity for a seeding and fertilizing applicator. *IFAC-PapersOnLine* **2018**, *51*, 536–540. [[CrossRef](#)]
22. He, W.; Liu, W.; Jiang, R.; Gu, Q.; Huang, J.; Zou, S.; Xu, X.; Zhou, Z. Control system design and experiments of UAV shot seeding device for rice. *Trans. Chin. Soc. Agric. Eng.* **2022**, *38*, 51–61. (In Chinese)
23. Liu, W.; Zhou, Z.; Xu, X.; Gu, Q.; Zou, S.; He, W.; Luo, X.; Huang, J.; Lin, J.; Jiang, R. Evaluation method of rowing performance and its optimization for UAV-based shot seeding device on rice sowing. *Comput. Electron. Agric.* **2023**, *207*, 107718. [[CrossRef](#)]
24. Liu, Y. A Thesis Submitted in Partial Fulfillment of the Requirements For the Degree of Master of Engineering. Master's Thesis, Huazhong University of Science and Technology, Wuhan, China, 2016. (In Chinese)
25. Li, Z.S. The Design of Butterworth Lowpass Filter Based on MATLAB. *Inf. Technol.* **2003**, *27*, 49–50. [[CrossRef](#)]
26. Gao, Y.; Xie, S. A Variable Step Size LMS Adaptive Filtering Algorithm and Its Analysis. *Acta Electron. Sin.* **2001**, *8*, 1094–1097. (In Chinese)
27. Kalman, R.E. A New Approach to Linear Filtering and Prediction Problems. *J. Fluids Eng.* **1960**, *82*, 35–45. [[CrossRef](#)]
28. Peng, D. Pseudo-linear Kalman Filter in Passive Target Tracking. *Softw. Guide* **2009**, *8*, 32–34.
29. Arianti, N.D.; Muslih, M.; Sitorus, A.; Bulan, R. Oscillation effect dataset on the measurement accuracy of load-cell sensor applied to the weigh basket. *Data Brief* **2021**, *38*, 107453. [[CrossRef](#)]
30. Ji, C. Study on Weighing Device for Seeding Amount of Tray in Rice Seedling Production Line. Master's Thesis, South China Agricultural University, Guangzhou, China, 2020. (In Chinese)

31. Gao, Y.; Zhao, H.; Zhu, Y.; Lou, J. The q-gradient LMS spline adaptive filtering algorithm and its variable step-size variant. *Inf. Sci.* **2024**, *658*, 119983. [[CrossRef](#)]
32. Liu, H. Design of the Weighting-principle-based Application Rate Measuring–Controlling System and Study of the Signal Processing Method. Master’s Thesis, Nanjing Agricultural University, Nanjing, China, 2019. (In Chinese)

Disclaimer/Publisher’s Note: The statements, opinions and data contained in all publications are solely those of the individual author(s) and contributor(s) and not of MDPI and/or the editor(s). MDPI and/or the editor(s) disclaim responsibility for any injury to people or property resulting from any ideas, methods, instructions or products referred to in the content.